ISSN: 0369-8963

Exploring Temperature-Dependent Electrical Conductivity, Seebeck Coefficient, and Figure of Merit of a novel Biocompatible Polypyrrole/ Agaricus bisporus (Edible Mushroom)/Zinc Oxide Composites for Thermal electric applications

Smitha M G[1], Mithun M S[2], Vijay S[2], Chandana S[2]

1. Department of Physics, Center of Excellence in Material Science and Devices, RNS Institute of Technology, Bengaluru- 560098, Karnataka, India

2. Department of Mechanical Engineering, RNS Institute of Technology, Bengaluru-560098, Karnataka, India

Abstract

The paper reports the analysis of the morphology, crystalline structure, and thermoelectric properties of a PolyPyrrole (PPy)/Agaricus bisporus (AB)/Zinc Oxide (ZnO) composite material intended for thermoelectric applications. Pure PPy and PPy/AB/ZnO composites with 10%, 20%, and 30% AB/ZnO were synthesized by in situ chemical oxidation method. The morphological structure and crystal structure are studied using Scanning Electron Microscope (SEM) and X-ray Diffraction spectroscopy (XRD) respectively. The images of SEM reveal that PPy exhibits a spherical continuous chain structure, ZnO with granular morphology, and the PPy/AB/ZnO composites display a blend of porous and granular structures. XRD analysis, performed over the 10°-80° range, indicates that pure PPy is amorphous, while the PPy/AB/ZnO composites are semi-crystalline. ZnO is confirmed to have a wurtzite hexagonal structure. Thermoelectric measurements conducted from room temperature to 100°C show that the Seebeck coefficient and power factor are highest for the PPy-10AB/ZnO composite, with values of approximately 61 μV/K and 573 $\mu V/m \cdot K^2$, respectively. Although its electrical conductivity is lower compared to other composites, the study demonstrates that the PPy/AB/ZnO composites exhibit properties comparable to those of existing lead-based thermoelectric materials. Consequently, these composites are environmentally friendly and show promise as alternatives in thermoelectric applications.

Keywords: Polypyrrole, Agaricus biporus, thermoelectric effect, Seebeck effect

Introduction

Analytical studies show that global energy is misspent as waste heat, underscoring the urgency for advancements in energy utilization. The need for efficient thermoelectric (TE) materials, capable of converting heat into electrical energy and vice versa, has garnered significant attention across the globe **[1]**. The need for eco-friendly material which is suitable for broad temperature ranges is in high demand. A key metric, the dimensionless figure of merit (ZT), serves as a benchmark for thermoelectric performance, with $ZT=(\alpha^2\sigma/\kappa)$ T. Achieving a high ZT necessitates maximizing both the Seebeck coefficient (α) and electrical conductivity (σ), while minimizing thermal conductivity (κ) to sustain the temperature differential driving the Seebeck effect **[2-4].**

 https://doi.org/10.5281/zenodo.14564269

In contemporary times, there's a growing focus on polymeric thermoelectric (TE) composites as potential alternatives to semiconductors like Bi_2Te_3 and PbTe. Polymers offer versatility, flexibility, excellent processability, and cost-effectiveness. However, polymer composites often exhibit subpar TE performance due to their limited electrical conductivity (σ). To address this issue, incorporating conductive fillers into polymer matrices can enhance their σ. Among conducting polymers, polypyrrole (PPy) has emerged as a particularly promising candidate for TE materials. Conducting polymers like PPy typically exhibit lower κ, simpler processability, flexibility, abundance, and lower manufacturing costs compared to semiconductor-based thermoelectric materials **[5-8]**. Carbon-based fillers are known to increase the performance of the thermoelectric materials. Therefore, we have chosen Agaricus biporus (Edible Mushroom) cap activated carbon black as filler. On the other hand, ZnO possesses a distinctive property that have surged in utilization as optoelectronic materials, sensors and as energy convertible materials **[9-10].**

This novel material PPy/AB/ZnO composites are environmentally friendly and show promise as alternatives in thermoelectric applications.

Methodology

I. Synthesis of Polypyrrole

Polypyrrole was synthesized via an in situ chemical oxidation method. Initially, pyrrole with a molar ratio of 0.3 M was mixed with 100 ml of distilled water in a round-bottomed flask containing a magnetic stirrer. The flask was then placed on an ice-filled tray to maintain a temperature range of 0 °C –5 °C. Subsequently, 0.6 M of ammonium persulfate (APS), an oxidizing agent, was dissolved in 100 ml of distilled water and added dropwise to the pyrrole solution from a burette. The reaction proceeded for 5 hours while maintaining the temperature between 0 °C and 5 °C.

Following the reaction, the black precipitate formed was purified by washing with acetone and filtration using a vacuum pump. The resulting precipitate was then dried in a hot air oven set to 100 °C. After reaching the desired temperature, the oven was turned off, and the sample was left overnight to ensure thorough drying.

The yield of the polypyrrole sample, measured using a digital weighing balance, was found to be 5 g considering it to be 100% weight percentage.

II. Carbonozation of Agaricus biporus (Edible mushroom)

The mushroom purchased from the local vendor is washed with distilled water to remove dirt. It is then cleaned with acetone for further purification. The mushroom cap is separated and dried in a hot air oven at 100 °C for 24 hours for the removal of water content in it. The complete dried sample is crushed to fine powder using mortar and pestle. The sample is preserved in an air-tight container for further studies. Figure 1 shows the carbonization of mushroom cap.

 https://doi.org/10.5281/zenodo.14564269

Fig 1.a. 1.b. 1.c 1.d

1.a Raw Mushroom, 1.b. separation of Mushroom cap,1.c Dried Mushroom at 100 °C for 24 hours, 1.d. Crushed and powdered mushroom

III. ZnO powder

ZnO powder (99% pure) was purchased from Aldrich (LR grade) and used as in its form.

IV. Synthesis of Polypyrrole/AB/ZnO composite material

PPy/AB/ZnO composites were synthesized using the in situ chemical oxidation method. Initially, pyrrole with a molar ratio of 0.3 M was mixed with 100 ml of distilled water in a round-bottomed flask containing a magnetic stir bar. The flask was then placed on an ice-filled tray atop a magnetic stirrer set to 400 rpm. Meanwhile, 0.6 M of ammonium persulfate (APS) dissolved in 100 ml of distilled water was prepared in a burette and added dropwise to the pyrrole solution.

Subsequently, 10% weight percent of AB and ZnO (assuming pyrrole weight as 100% weight percentage) powder was added to the mixture. The reaction proceeded for 5 hours at a temperature maintained between 0 ℃ and 5 °C. The resulting black precipitate was purified with acetone, filtered using a vacuum pump, and dried in a hot air oven at 100 °C for 3 hours. The dried powder was then subjected to a muffle furnace for 2 hours, ground, and stored for further analysis.

The yield of the PPy/AB/ZnO composite was measured and found to be 3.2 g. The same procedure was repeated with varying weight percentages of AB/ZnO powder (20%, 30%) added to PPy to obtain PPy/AB/ZnO-20, PPy/AB/ZnO-30 composites, respectively.

Characterization

1.SEM Analysis

The morphology of the samples was examined using a Scanning Electron Microscope (SEM), (Vega3 TESCAN). Figure 2. a-d presents SEM micrographs depicting pure PPy, pure AB, pure Zno and PPy/AB/ZnO-30% composites. The SEM images reveal that PPy has a spherical structure, while pure AB has porous, and pure ZnO has granular structures while PPy/AB/ZnO-30% composites show agglomerated structures with voids.

Furthermore, it is evident from the images that as AB/ZnO particles are incorporated into the PPy chain, more clusters of PPy form, accommodating the particles. Consequently, this leads to a

https://doi.org/10.5281/zenodo.14564269

reduction in the length of the polymer chain along with a decrease in the volume fraction. These observations confirm the formation of PPy/AB/ZnO composites.

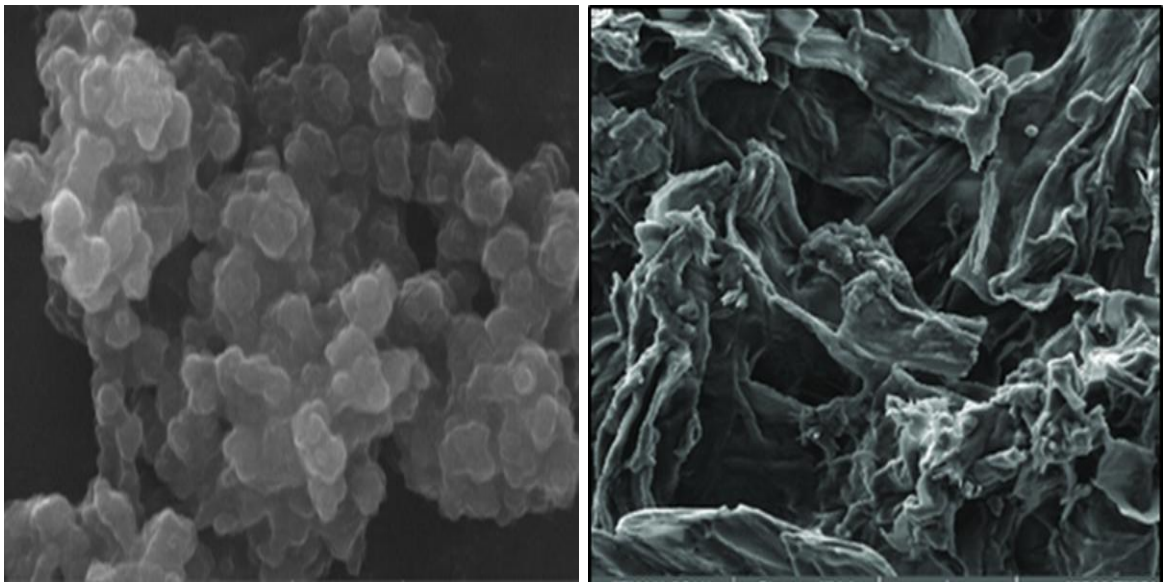

Fig 2.a. SEM image of pure PPy b. SEM image of Mushroom cap powder

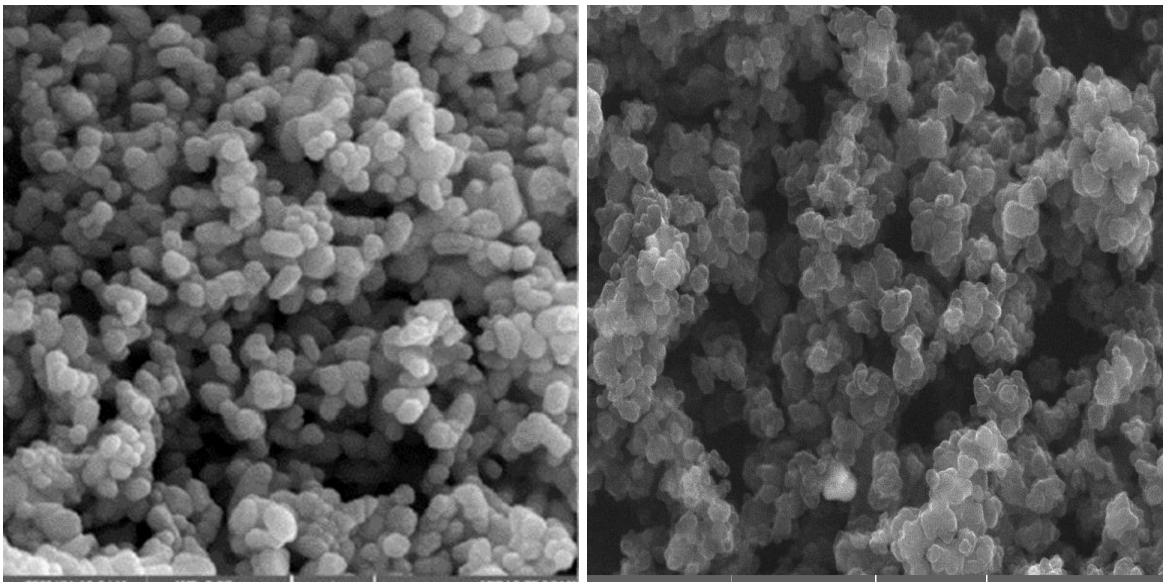

c. SEM image of ZnO powder d. SEM image of PPy/AB/ZnO - 50% composites

2. XRD analysis

The crystal structures of PPy, AB, and PPy/AB/ZnO composites were investigated using an X-ray diffractometer (XPERT-3). The analysis was conducted at a 2θ angle ranging from 10° to 80° with a step-wise variation of 0.03° in continuous mode. Copper K-alpha X-rays with a wavelength of 1.54 Å were employed for the analysis. The XRD images of the compounds are shown in Figure

https://doi.org/10.5281/zenodo.14564269

3. From the image, it is observed that XRD of pure PPy has an amorphous structure, with a smooth hump at 25°. The composites of PPy/AB/ZnO are also displayed. The following table shows the peak position and their d-spacing for both PPy/AB/ZnO –20 and PPy/AB/ZnO-30 composites.

Table 1: D-spacing of PPy/Ab/ZnO composites

Compound	Peak Position	d-Spacing (Å)
PPy-20 ZnO-AB	43.6965º	2.06987Å
	48.993º	1.85776Å
	51.0742º	1.78684Å
	72.5225º	1.30235Å
	75.5855º	1.25700Å
PPy-30 ZnO-AB	43.7349º	2.06814Å
	49.0712º	1.85499Å
	51.2688º	1.7805Å
	72.5269º	1.30228Å
	75.2894º	1.26121Å

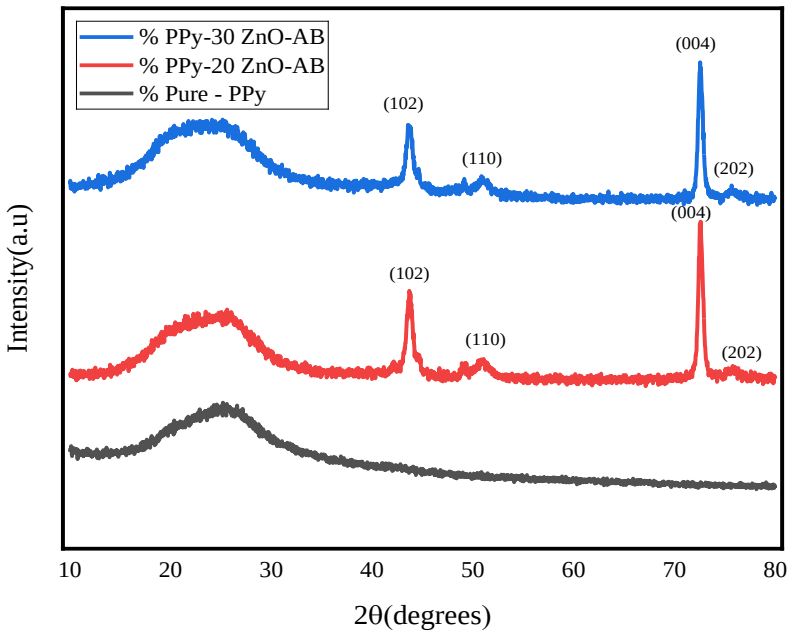

Fig.3. XRD spectrum of Pure and PPy-ZnO-AB composites

Pellet Preparations

The pellets of pure PPy and PPy composites were fabricated using 0.15 g of powder each. The powder was placed into a die and compressed with a hydraulic press under 10 tons of pressure. The thickness of the resulting pellets was measured with a digital screw gauge, showing a range from 1.542 mm to 1.605 mm. These pellets were then employed to investigate the thermo-electric properties of the materials.

https://doi.org/10.5281/zenodo.14564269

The thermal behavior of the samples was studied from room temperature to 100 ^{o}C using two probe thermo couple apparatus at constant current of 1mA.

3. Thermal Studies

i. Study of Electrical conductivity of the sample.

The study of electrical conductivity gives the insight about the transportation of the charge carriers. It also gives the information about the nature of the material. In our study, we have studied the variation of electrical conductivity at constant current. The variation of voltage with respect to temperature is recorded and then the electrical conductivity of the sample is calculated using the formula

$$\sigma = \frac{d}{R*A} \qquad \text{..... (1)}$$

Where d is the thickness of the sample in m, R is the resistance of the sample in Ω, A is the area of the sample in m^2.

The plot of variation of electrical conductivity with temperature is shown in the figure 4.

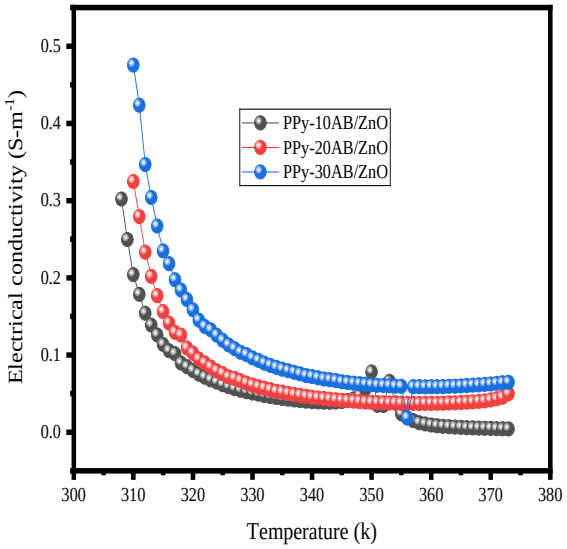

Fig.4. Electrical conductivity of PPy/AB/ZnO composites

From Figure 4, we observe that electrical conductivity is high in the room temperature and decreases and becomes almost constant at high temperatures. The reason attributed is that the vibration of metal ion (ZnO) increases with temperature which intern decreases the conductivity, also the majority of the charge carriers may already be excited leading to saturation point beyond which there is no significant increase in the carrier concentration.

ii. EMF studies

A material's Seebeck coefficient (also known thermoelectric power, and thermoelectric sensitivity) is a measure of the magnitude of an induced thermoelectric voltage in response to a temperature difference across that material. We have studied the variation of EMF generated with increase in

https://doi.org/10.5281/zenodo.14564269

temperature. The setup used for the measurement is shown in figure 5. One apparatus was set to room temperature while the other recorded temperature variations. The current was fixed at 1 mA and voltage changes were measured for each degree raise in the temperature.

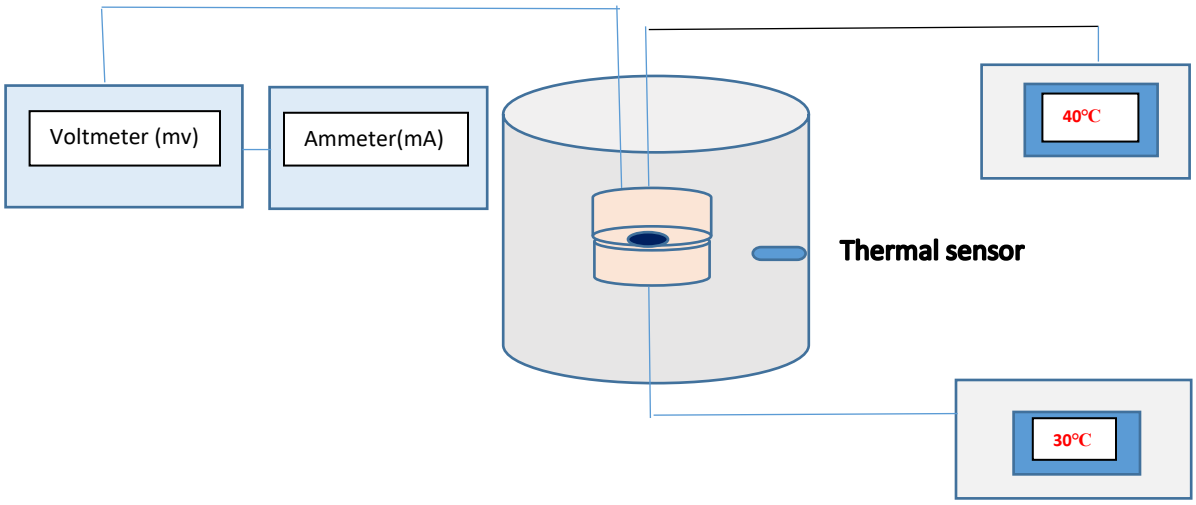

Fig. 5. Schematic diagram of thermos electric measurement apparatus

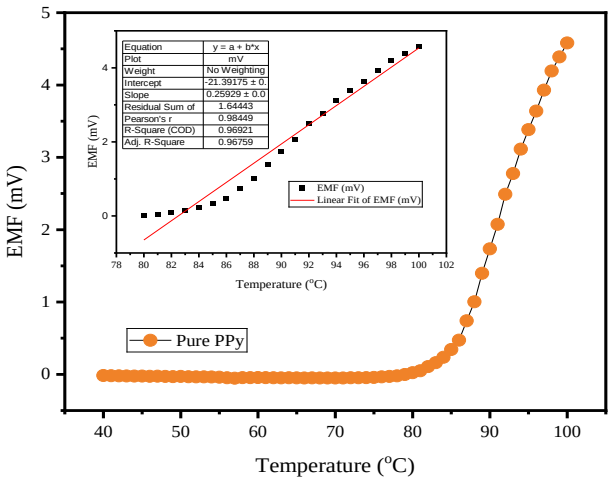

Fig 6.a. V/T plot of PPy

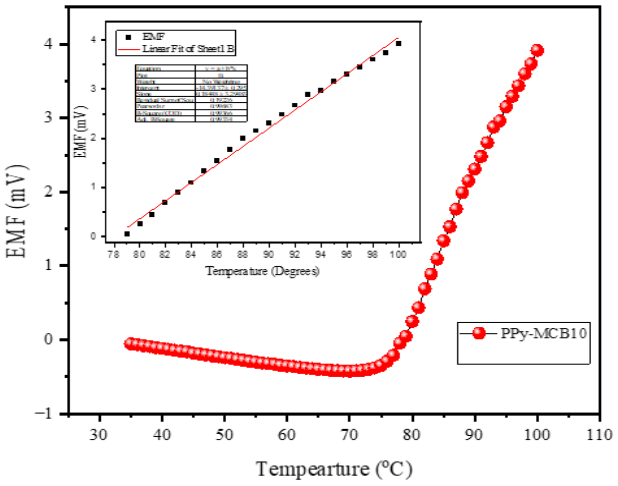

b. Linear plot of PPy/AB/ZnO-10%

https://doi.org/10.5281/zenodo.14564269

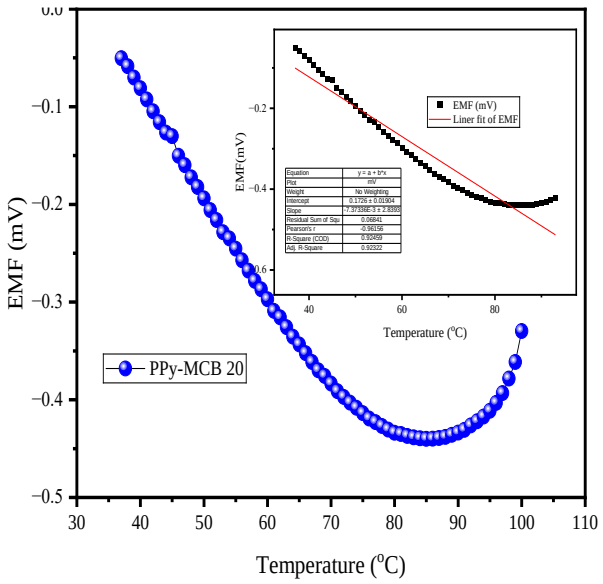

c. V/T plot of PPy/AB/ZnO-20%

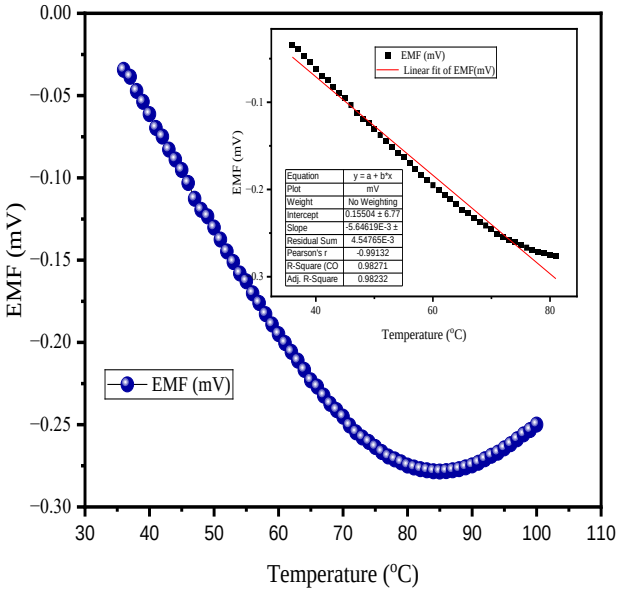

d. Linear plot of PPy/AB/ZnO-30%

Figures 6.a, b, c and d show the variation of voltage with respect to temperature. Inset shows the linear fit plots of the respective compound. The plots reveal that all compound PPy and PPy/AB/ZnO composites show n-type semiconductors up to 80 °C, beyond which it flips to p-type semiconductor. The reason attributed is that, as the temperature increases, the charge carrier diffusion and phonon drag takes place. Also, the influence of ZnO will contribute electrons which becomes the majority charge carriers **[11-13].**

iii. Seebeck Coefficient and power factor studies of PPy-AB/ZnO composites

The efficiency of energy conversion relies on the thermoelectric materials used. The Seebeck coefficient was calculated for 5°C difference in the temperature using the formula as given in eq (2).

$$S = - \Delta V / \Delta T \qquad \text{……. (2)}$$

Where S is the Seebeck coefficient is volts per kelvin (μV/K), ΔV (mV) and ΔT (k) are the voltage and temperature difference respectively. The power factor is calculated using the eq (3)

$$P.F = S^2 \sigma \qquad \text{……(3)}$$

Where S is the seebeck Coefficient (μV/K) and σ is the electrical conductivity ($S\text{-}m^{-1}$)

Figures 7 and 8 are the plots of Seebeck Coefficient and power factor of PPy/AB/ZnO composites respectively. From the plot 7, we observe the increase in Seebeck coefficient with temperature. The reason is attributed as the result of the introduction of additional interfacial energy barriers in the grafted conducting network, which inhibit low-energy carriers from moving across the interfaces. Potential energy barriers at the interfaces preferentially allow high-energy carriers to pass through, resulting in enhanced scattering of low-energy carriers **[14-18].** Figure 8 is the plot

https://doi.org/10.5281/zenodo.14564269

of power factor variation with temperature. From the plot we observe that PPy-10AB/ZnO has higher power factor when compared to PPy-20AB/ZnO and PPy-30AB/ZnO. The highest power factor at 373k for PPy-10AB/ZnO is 570μW/mk^2.

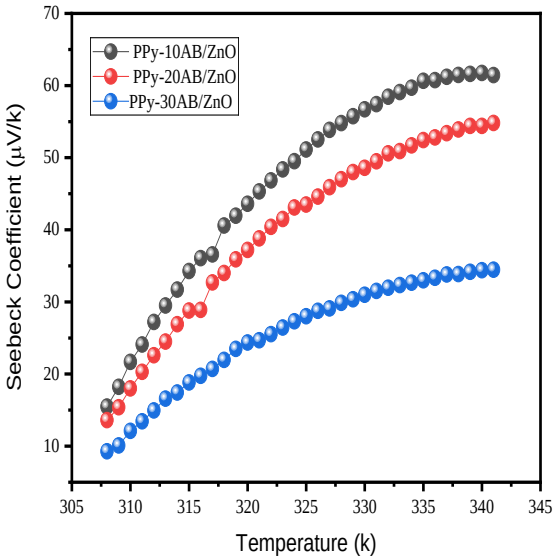

Fig.7. Seebeck coefficient of PPy/AB/ZnO composites with temperature

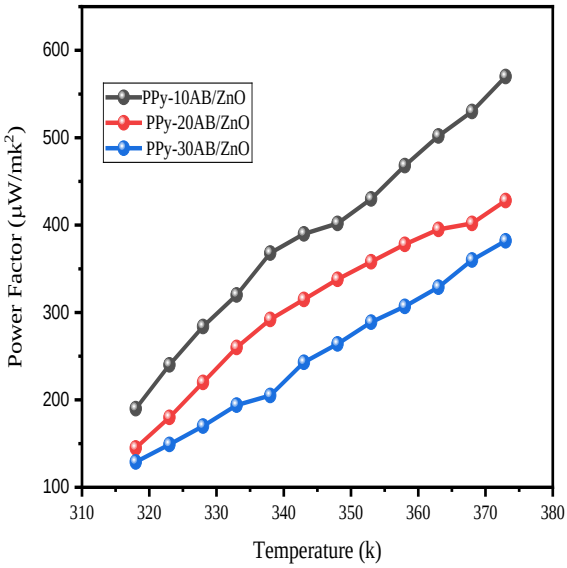

Fig.8. Power factor PPy/AB/ZnO composites with temperature

iv. Figure of merit studies

The performance of these materials is quantified by a dimensionless parameter called the figure of merit (zT), The corresponding formula is given by

$$ZT = s^2 \sigma T/k \quad \ldots\ldots\ldots\ldots\ldots\ldots (4)$$

where *S* represents the Seebeck coefficient, σ denotes the electrical conductivity, *T*is the absolute temperature, and *k* stands for thermal conductivity.

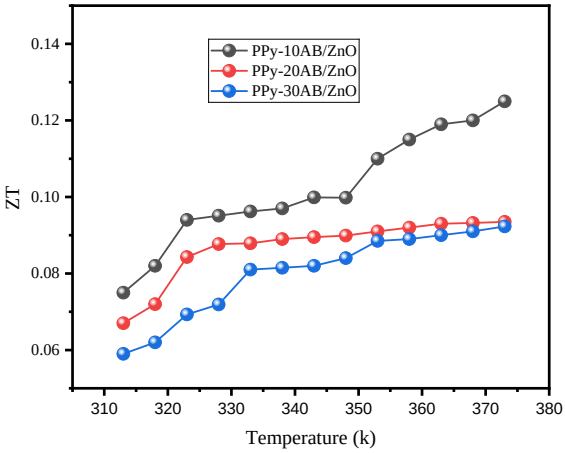

Fig.9. ZT variation of PPy/AB/ZnO composites with temperature composites with temperature

https://doi.org/10.5281/zenodo.14564269

Figure 9 shows the figure of merit (zT) as a function of temperature for all the prepared samples. For each composite, the zT value increased gradually with temperature. The highest zT observed was 0.12 at 373 K for the PPy-10AB/ZnO composite. This increase could be attributed to reduced agglomeration and the enhanced surface area resulting from the incorporation of AB, which is highly porous **[18-20]**.

Conclusion

We have successfully synthesized the compound viz pure PPy, PPy/AB/ZnO composite using in situ chemical oxidation method. The SEM and XRD of the compounds reveal spherical/ fibrous/Agglomerated structures for pure PPy/ pure AB/ PPy/AB/ZnO composites respectively. XRD of AB shows peaks revealing the presence of metallic compounds in the mushroom cap and the composites of PPy/ AB/ZnO composites show a semi-crystalline structure. The Seebeck coefficient measurements, taken from room temperature to 100 °C, show that up to 80 °C, the material behaves as an n-type semiconductor, and beyond that temperature, it transitions to a p-type semiconductor. Among the samples, the PPy-10AB/ZnO composite demonstrates superior performance, with a Seebeck coefficient of 61 μV/K, a power factor of 570 μW/mK², and a figure of merit of 0.12 373k. PPy-based composite could serve as an effective polymeric thermoelectric material, offering an environmentally friendly alternative to lead-based composites.

References

1. Kanatzidis MG. “Nanostructured thermoelectrics: the new paradigm?”, Chem Mater. 2010; 22,3,648-659.
2. LaLonde AD, Pei YZ, Wang H, Snyder GJ, “Lead telluride alloy thermoelectrics”, Mater Today, 2011,14,526-532.
3. Sootsman JR, Chung DY, Kanatzidis MG, “New and old concepts in thermoelectric materials”, Angew Chem Int Ed, 2009,48,8616-8639.
4. He JQ, Kanatzidis MG, Dravid VP, “High-performance bulk thermoelectrics via a panoscopic approach”, Mater Today, 2013,16,166-76.
5. Zhao LD, Dravid VP, Kanatzidis MG, “The panoscopic approach to high-performance thermoelectrics”, Energy Environ Sci, 2014,7,251-68.
6. Cheng, H.; He, X.; Fan, Z.; Ouyang, J, “Flexible Quasi-Solid State Ionogels with Remarkable Seebeck Coefficient and High Thermoelectric Properties”, Adv. Energy Mater, 2019, 9, 1901085.
7. Lu, Y.; Yu, Z.-D.; Zhang, R.-Z.; Yao, Z.-F.; You, H.-Y.; Jiang, L.; Un, H.-I.; Dong, B.-W.; Xiong, M.; Wang, J.-Y.; Pei, J, “Rigid Coplanar Polymers for Stable n-Type Polymer Thermoelectrics”. Angew. Chem., Int. Ed. 2019, 58, 11390– 11394,
8. Liang, L.; Fan, J.; Wang, M.; Chen, G.; Sun, G, “Ternary thermoelectric composites of polypyrrole/PEDOT: PSS/carbon nanotube with unique layered structure prepared by one-dimensional polymer nanostructure as template”. Compos. Sci. Technol. 2020, 187, 107948.

 https://doi.org/10.5281/zenodo.14564269

9. S.D. Ponja, S. Sathasivam, I.P. Parkin, C.J. Carmalt , “Highly conductive and transparent gallium doped zinc oxide thin films via chemical vapor deposition”, Sci. Rep,2020, 10 , 638.
10. Y.-P. Lee, Ch-Ch Lin, Ch-Ch Hsiao, P.-A. Chou, Y.-Y. Cheng, Ch-Ch Hsieh, Ch-A. Dai “Nanopiezoelectric devices for energy generation based on ZnO nanorods/flexible-conjugated copolymer hybrids using all wet-coating processes”, Micromachines, 2020,11 1, 14.
11. Liang, L.; Chen, G.; Guo, C.-Y, “Enhanced thermoelectric performance by self-assembled layered morphology of polypyrrole nanowire/single-walled carbon nanotube composites. Compos. Sci. Technol. 2016, 129, 130–136.
12. Sourav Mondal, Debasis Dhak, Bidyut Saha, “Polymer and composite based thermoelectrics: Basics, scopes and issues”,Vietnam J.Chem,2022,60,6,689-699.
13. Zhang, Z.; Chen, G.; Wang, H.; Li, X, “Template-directed in situ polymerization preparation of nanocomposites of PEDOT:PSS-coated multi-walled carbon nanotubes with enhanced thermoelectric property”, Chem. Asian J. 2015, 10, 149–153.
14. 12. Zhang, Z.; Chen, G.; Wang, H.; Zhai, W. Enhanced thermoelectric property by the construction of a nanocomposite 3D interconnected architecture consisting of graphene nanolayers sandwiched by polypyrrole nanowires. J. Mater. Chem. C. 2015,3, 1649–1654.
15. 13. Li, J.; Du, Y.; Jia, R.; Xu, J.; Shen, S.Z, “Flexible thermoelectric composite films of polypyrrole nanotubes coated paper”. Coatings, 2017, 7, 211.
16. 14. Wu, J.; Sun, Y.; Pei, W.-B.; Huang, L.; Xu, W.; Zhang, Q, “Polypyrrole nanotube film for flexible thermoelectric application”. Synth.Met. 2014, 196, 173–177.
17. Culebras, M.; Uriol, B.; Gómez, C.M.; Cantarero, A, “Controlling the thermoelectric properties of polymers: Application to PEDOT and polypyrrole”, Phys. Chem. Chem. Phys. 2015, 17, 15140–15145.
18. 16. Zhang, W.-D.; Xiao, H.-M.; Fu, S.-Y, “Preparation and characterization of novel polypyrrole-nanotube/polyaniline free-standing composite films via facile solvent-evaporation method”, Compos. Sci. Technol. 2012, 72, 1812–1817.
19. 17. Song, H.; Cai, K.; Wang, J.; Shen, S,“Influence of polymerization method on the thermoelectric properties of multi-walled carbon nanotubes/polypyrrole composites”, Synth. Met. 2016, 211, 58–65.
20. 18. Baghdadi, N.; Zoromba, M.S.; Abdel-Aziz, M.H.; Al-Hossainy, A.F.; Bassyouni, M.; Salah, N, “One-Dimensional Nanocomposites Based on Polypyrrole-Carbon Nanotubes and Their Thermoelectric Performance”, Polymers 2021, 13, 278.

 https://doi.org/10.5281/zenodo.14564269